REPORT DOCUMENTATION PAGE

Form Approved
OMB NO. 0704-0188

AGENCY USE ONLY *(leave blank)*	2. REPORT DATE	3.REPORT TYPE AND DATES COVERED
	July 12, 1998	Final 1992-98

4. TITLE AND SUBTITLE
High Pressure Spectroscopic studies of AlGaAs, GaAs, and II-VI and other semiconductors and heterostructures.

5.FUNDING NUMBERS
DAALO3-92-G-0381

6. AUTHORS
M. Chandrasekhar

7. PERFORMING ORGANIZATION NAMES AND ADDRESSES
Physics Department, University of Missouri, Columbia MO 65211

8. PERFORMING ORGANIZATION REPORT NUMBER

9. SPONSORING /MONITORING AGENCY NAMES AND ADDRESSES
U.S. Army Research Office
P.O. Box 12211
Research Triangle Park, NC 27709-2211

10. SPONSORING /MONITORING AGENCY REPORT NUMBER
ARO 29682.20-PH

11.SUPPLEMENTARY NOTES
The views, opinions and findings contained in this report are those of the authors and should not be construed as an official Department of the Army position, policy or decision, unless designated by other documentation.

12a. DISTRIBUTION / AVAILABILITY STATEMENT
Approved for public release; distribution unlimited.

12b DISTRIBUTION CODE

13. ABSTRACT *(Maximum 200 words)*

We summarize our work over the last five years on high pressure studies using optiucal techniques such as photoluminescence, photoreflectance and Raman scattering of GaAs/AlAs superlattices, polycrystalline and amorphous powder samples of phenylene-type polymers and oligomers, ordered and disordered $GaInP_2$, and ZnCdSe heteostructures. In order to modulate interatomic electronic interactions in the conventional semiconductors and to study both intrachain and interchain interactions in the conjugated polymers,these investigations were performed at hydrostatic pressures up to 70 kbar and in a temperature range of 20 to 300 K. We report characteristic changes of the emission spectrum which depend on both the molecular environment as well as the intramolecular bond configuration.

14. SUBJECT TERMS

15. NUMBER OF PAGES
27 (including this page)

16.PRICE CODE

17. SECURITY CLASSIFICATION OF REPORT:	18.SECURITY CLASSIFICATION OF THIS PAGE	19. SECURITY CLASSIFICATION OF ABSTRACT	20. LIMITATION OF ABSTRACT
UNCLASSIFIED	UNCLASSIFIED	UNCLASSIFIED	UL

Table of Contents

High Pressure Spectroscopic studies of AlGaAs, GaAs, and II-VI and other semiconductors and heterostructures.

Final Report, 1998

Meera Chandrasekhar
Physics Department
University of Missouri, Columbia MO 65211

I. Introduction

The last decade and a half has seen numerous breakthroughs in optoelectronic and microwave devices, fueled by the development of high quality ternary semiconductors. Laser diodes, bipolar transistors, charge coupled devices, superlattice photodetectors and picosecond photodetectors are a few of many examples. The alloys and their quantum well heterostructures (QWH) are versatile: their band gaps can be tailored by changing the alloy composition or the well widths in the QWH, and tuned to match a specific application.

Pressure, coupled with optical techniques has long been recognized as an indispensable tool in the study of semiconductors. This powerful and fundamental thermodynamic tool has the advantage of providing a 'clean' technique for changing bond distances, and consequently the electronic properties. An interesting example of the predictive power of pressure was seen in the development of high Tc materials. The fact that a smaller atom was needed to increase Tc was inferred after a pressure measurement showed that squeezing the atoms closer together increased Tc. Another example is seen in the frequently used (Ga,Al)As alloys, where changes in the conduction bands (CB's) due to alloying are mimicked by pressure: the direct Γ CB increases in energy and crosses the X CB, both with increasing pressure and with increasing Al content. The advantage with pressure is that the studies can be made on one single sample, without the vagaries of dopant concentration, alloy disorder effects, etc., which can occur for samples of different compositions.

The PI has amassed a considerable body of work in high pressure studies of quantum well systems using low temperature photoluminescence (PL) and photoreflectance (PR) in a diamond anvil cell. The two techniques are complementary: PL enhances the lowest confined transitions in

QWH and is excellent for impurity related transitions. PR is ideal to study higher quantized levels in the QWH. Ours is the first laboratory to use PR under pressure in the QWH, and, to our knowledge, we are the only laboratory in the world with this capability. In the past few years, we have studied the GaAs/AlGaAs, GaSb/AlSb, GaAs/InGaAs QWH, and the ZnSe/GaAs and ZnSe/ZnCdSe systems. We have used pressure to obtain the valence band offset, shown that the pressure coefficients of the confined transitions depend on the well width (using PL) and on the quantum number, of the transition (using PR).

Quantum well heterostructures of the II-VI binary and ternary compounds offer an exciting array of band gaps and physical properties. The band gaps range from the deep red to the near UV region (1.6 to 3 eV) by using Cd and Zn for the Group II and Se, Te and S for the Group VI material. Continuous tuning of the band gap is achieved by means of ternary alloys or by replacing the Group II with a magnetic ion such as Mn or Fe, which produces interesting magnetic effects in these diluted magnetic semiconductor (DMS) alloys. QWH such as $ZnSe/Zn_{1-x}Cd_xSe$, $Cd_{1-x}Mn_xTe$ / $Cd_{1-y}Mn_yTe$ and various other combinations have been successfully grown by MBE. They have been studied via photoluminescence, piezo-, electro-, and photo-modulated reflectivity spectra. Virtually all of them are strain layered structures, grown on a GaAs substrate.

Applications of the II-VI heterostructures range from the newest room temperature blue-green lasers (announced by the 3M company), modulators, nonlinear devices, optical memories and flat panel high resolution displays and screens (manufactured by Sharp, Japan). The shorter wavelengths are favored because the lower diffraction allows better focusability. Laser layouts have been made with 2 million lasers/cm^2, triggered with blue light.

A recent entrant into the field of opto-electronic device materials is the family of conjugated polymers. Conjugated polymers are characterized by highly delocalized-electronic structure along the polymer backbone. Undoped conjugated polymers behave as semiconductors with band gaps of 1.4-3 eV. When suitably doped, these materials can display metallic conductivities. The promise of conducting polymers is to combine the chemical, mechanical, and processing properties of plastics with the electrical behavior of metals and semiconductors. Applications of conducting polymers include capacitors, cable shielding, electrochromic smart-windows, rechargeable batteries and sensors. In recent years considerable interest has been directed towards undoped conjugated polymers as replacements for conventional semiconductors in optical devices,[1,2,3,4,5]

---

[1] J.H. Burroughes, D.D.C. Bradley, A.R. Brown, R. Marks, K. Mackay, R.H. Friend, P.L. Burn, and A.B. Holmes, Nature **347**, 539 (1990).
[2] D. Brown, and A.J. Heeger, Appl. Phys. Lett. **58**, 1982 (1991).
[3] N.C. Greenham, S. Moratti, D. C Bradley, R.H. Friend, and A.B. Holmes, Nature **355**,628 (1993).
[4] G.J. Denton, N. Tessler, N.T. Harrison, R.H. Friend, Phys. Rev. Lett. **78**, 733 (1997).

driven by the promise of cheap, readily processible for light emitting diodes, computer screens, and lasers.

This report is organized as follows: In Sec. II we review our recent work on short period GaAs/AlAs superlattices. In Sec. III we present our recent work on conjugated polymers. In Sec III. we present our work on polarized photomodulated reflectivity and photoluminescence studies of ordered $InGaP_2$, and in Sec. V we review our comparative study of ordered and random alloy quantum wells of $Zn_{1-x}Cd_xSe/ZnSe$ under pressure. Sec. VI lists the papers published with the help of this grant. Sec. VII lists the personnel supported by this grant.

II. Photoluminescence of Short Period GaAs/AlAs Superlattices

Carrier dynamics and recombination mechanisms in semiconductor superlattices, in particular those with a staggered band alignment, have been the subject of many investigations. High quality superlattices comprising alternating layers of GaAs and AlAs fabricated by epitaxial techniques with monolayer precision are of much interest, thanks to the possibility of designing many physical situations that develop as a result of dimensional changes. Combined with external perturbations such as temperature and pressure, one can tune the electronic states with respect to one another, thus revealing the nature and extent of various interactions.[6]

When alternating slabs of GaAs and AlAs are grown epitaxially on a (typically (001) oriented) GaAs substrate, the band alignment at the interfaces leads to potential wells for the electrons and holes. The conduction band minima associated with the Γ-point in GaAs and AlAs form potential wells for electrons in GaAs slabs. Similarly, the potential wells in the valence band for holes (only heavy hole bands are shown) reside in GaAs slabs. The potential wells for electrons formed at the X-point conduction minima, however, reside in AlAs slabs. This staggered or type-II alignment has the novel feature that recombination of charge carriers across the heterointerface provides a new channel, often in competition with the usual type-I transition across the valence and conduction sub-bands in GaAs. For a given superlattice structure, the difference in energy between the type-I and type-II transition, can be tuned with external hydrostatic pressure in a continuous and reversible manner, thus enabling an elucidation of the properties of various interband transitions. Another motivation for pressure studies is to gain insight into intervalley

[5] N. Tesslers, G.J. Denton, and R.H. Friend, Nature **382**, 695 (1996).

[6]See for example, S. Adachi, GaAs and related materials: Bulk Semiconducting and Superlattice Properties, World Scientific, Singapore 1994.

scattering rates[7,8] which play an important role in relaxation of photo-excited carriers and high field transport.

This segment of the report is structured as following: Section IIa describes our experimental setup. In Sec. IIb we show that the temperature dependence of the interband excitonic transition energies can be fitted very well with a Bose-Einstein type equation which was proposed by Viña *et al*[9] to explain the temperature dependence of energy bands in Ge. In Sec. IIc we focus on the pressure dependence of type-I and type-II transitions. The results on the PL linewidths as a function of pressure are presented. We calculate the intervalley electron-phonon deformation potential from our experimental results and show that the deformation potential changes with temperature which till now had only been predicted theoretically.

IIa . Experimental Setup

The $(GaAs)_m/(AlAs)_m$ superlattices with m=4, 5,10 and 20 were grown on a (001) GaAs substrate by molecular beam epitaxy (MBE), growth temperatures being 600°C. The (10,10) and the (20,20) superlattice were studied under hydrostatic pressure employing a diamond anvil cell (DAC); for these measurements, the substrates were thinned to total thickness of ~50 mm. Argon was used as a pressure transmitting fluid in the DAC. Pressure (P) was measured using the luminescence of a ruby chip located in the pressure chamber. The PL signature from the GaAs substrate also serves as a good calibration for pressure since the direct band gap of GaAs moves at the rate of 10.7 meV/kbar. The PL spectra were excited using the 514.5 nm (m=5, 10, 20) and 457.9 nm (m=4) lines of an Ar^+ laser. The emitted radiation was analyzed with a SPEX 0.85m double monochromator equipped with a cooled GaAs photomultiplier tube and standard photon counting electronics. For the low temperature work with DAC a closed cycle helium refrigerator was employed. The temperature dependence of PL at ambient pressure and in the temperature range 5 to 300 K was investigated with a variable temperature cryostat.

IIb. Temperature Dependence Of Transition Energies

For $(GaAs)_{10}/(AlAs)_{10}$ the type-I and type-II transitions lie very close. For this sample, the

---

[7]S. Satpathy, M. Chandrasekhar, H.R. Chandrasekhar and U. Venkateswaran, Phys. Rev. B **44**, 11339 (1991).

[8]S. Zollner, S. Gopalan and M. Cardona, Appl. Phys. Lett. **54**, 614 (1989); J. Appl. Phys. **68**, 1682 (1990); Solid State Commun. **76**, 877 (1990).

[9]L. Viña, S. Logothetidis, and M. Cardona, Phys. Rev. B **30**, 1979 (1984).

type-II transition is dominant in the low temperature PL; at higher temperatures, the quantum confined Γ-level is increasingly populated, resulting in the corresponding increase in the intensity of the type-I transition. The PL spectrum of the (10,10) superlattice at 70, 105, and 120 K shows the appearance of the high energy peak E^I at the highest temperature (Fig. 1). With increasing temperature the intensity of the low energy peak (E^{II}) decreases and finally only E^I is observed above 180 K.

We have studied the temperature of the type-I and type-II transitions from the photoluminescence (PL) spectra in a series of $(GaAs)_m/(AlAs)_m$ (for m=5, 10 and 20) superlattices show that the temperature dependence of energy bands can be described very well with a Bose-Einstein type equation. From these measurements the parameters that describe the temperature dependence of excitonic transition energies and the corresponding broadening of the PL line are deduced.

IIc. Pressure Dependence Of The Transition Energies

Figure 2 shows a typical PL spectra of $(GaAs)_{20}/(AlAs)_{20}$ measured at 16 K under hydrostatic pressure. The superlattice is type-I at atmospheric pressure and transforms into type-II at 5 kbar as signaled by the emergence of the type-II peak. Above this pressure the superlattice is pseudo-direct and the intensity of the type-I transition decreases. With an increase in pressure the high energy peak (type-I) shifts rapidly to higher energies and the low energy peak (type-II) moves to lower energies. Type-II emission is not observed below the crossover pressure in the PL spectra. The pressure shifts of the two transitions for the (20,20) superlattice are shown in Fig. 3. The type-I and type-II transitions exhibit a linear pressure coefficient of 10.1 meV/kbar and -2.5 meV/kbar, respectively, the type-I - type-II crossover occurring at ~5 kbar.

Similar measurements on the (10,10) superlattice displayed in Fig. 3 show that at atmospheric pressure, it is a type-II, the Γ-X crossover having already occurred and the energy of the pseudo-direct transition thus being lower in energy than that of the direct transition. At P=0, both type-I and type-II are observed in the PL. Type-I emission shows a blue shift of 10.4 meV/kbar whereas the type-II emission is red shifted by -2.1 meV/kbar. The (10,10) superlattice has higher energies for both type-I and type-II levels compared to the (20,20) superlattice as a result of the increased confinement with decrease in the superlattice period.

The type-I excitonic line in the PL spectrum of GaAs/AlAs superlattice is broadened by the hybridization of the Γ exciton with the X and the L continua via electron-phonon coupling. Under

external pressure, the Γ conduction minimum moves up in energy and crosses the bottom of the L and X conduction bands of the AlAs layer. The coupling between the Γ exciton and the X and L continuum via intervalley scattering of the electron broadens the Γ exciton level observed in PL. Figure 4 shows the broadening ΔΓ (difference between the actual and average linewidth below crossover pressure) vs. the energy separation between g_Γ and g_X at three different temperatures for $(GaAs)_{20}/(AlAs)_{20}$. The crossover pressure P_c is defined as the pressure when the type-I and type-II transitions have the same energy ($g_\Gamma=g_X$). The PL line shapes were fit with Gaussians. We find that the linewidth increases monotonically as the density of continuum states increases, following roughly the $(g_\Gamma-g_X)^2$ dependence. For all three temperatures, the linewidth almost remains constant below crossover pressure. We fit the linewidth above crossover by a square root function. It is observed that the square root function changes as a function of temperature. From the fits we obtain the function $\Delta\Gamma/\sqrt{\varepsilon-\varepsilon_x}$ and using a well known equation for the deformation potential (D) as a function of the PL line width we calculate $D_{\Gamma X}$ (intervalley deformation potential between the Γ valley and the X valley). At 16K we obtain $D_{\Gamma X}$=5.2eV/D, at 75K, $D_{\Gamma X}$=7.3eV/D and at 100K, $D_{\Gamma X}$=8.2eV/D.

The temperature dependence of the deformation potential is consistent with the theory of Zollner *et al.*[10] where the *effective* deformation potential is temperature dependent. This takes into account the contribution from the TA phonons. To our knowledge this is the first time that the temperature dependence of the intervalley potential for GaAs quantum wells/superlattices has been experimentally observed.

III. Optical Spectroscopy of Conjugated Polymers

The emission of light by polymers in an electric field (electroluminescence) was first demonstrated in poly (p-phenylene vinylene) (PPV), in 1990. Significant progress has been made in improving the efficiency and the range of available emitted colors. Ladder poly (p-phenylene)

[10]S. Zollner, S. Gopalan and M. Cardona, Appl. Phys. Lett. **54**, 614 (1989); J. Appl. Phys. **68**, 1682 (1990); Solid State Commun. **76**, 877 (1990).

(LPPP) have been found to be attractive candidates for blue light emitting diodes (LED's)[11,12,13] and other devices due to their high photoluminescence yields. The oligomer para hexaphenyl (PHP) has also been successfully applied to create the elements for a red-green-blue color display.[14]

We have conducted optical studies, using primarily photoluminescence (PL), Raman scattering, absorption and photoinduced absorption (PIA) spectroscopies to investigate the electronic and vibrational states of chosen polymers beginning with para hexaphenyl (PHP) and methyl substituted ladder poly para phenylene (m-LPPP) as models of chain and ladder polymers. PHP is known to form monoclinic crystallites and is characterized by a torsional degree of freedom between neighboring phenyl rings. m-LPPP on the other hand is planar due to the methyl bridge connecting two adjacent benzene rings which suppresses the rotational degree of freedom between adjacent rings. The primary focus of this work has been to perform these studies under hydrostatic pressure in a diamond anvil pressure cell. By applying up to 100 kbar at temperatures of 10 to 300K, we were able to probe inter-and intrachain interactions by using pressure as the parameter that changes interatomic distances and thus tunes the structural and electronic properties of polymer chains.

This segment of the report is structured in the following way; Section IIIa describes of the experimental setup. In Section IIIb the electronic properties of m-LPPP and PHP under pressure are presented. This includes PL, absorption under high pressure. Section IIIc consists of the Raman scattering results of PHP including studies under high pressure. Planarization effects in PHP and a comparison of the electronic and Raman spectra between experiment and theory are discussed.

IIIa Experimental Setup

The raw materials were provided in powder form by Tokio Chemical industries Ltd. and MPI for Polymerforschung. In order to investigate the different samples under hydrostatic pressure, diamond anvil cells (DAC) with preindented stainless steel gaskets were used. Argon was used as a pressure transmitting fluid in the DAC. Pressure (P) was measured using the luminescence of a ruby chip located in the pressure chamber. The pressure range used in this work was between 0 and 70 kbar. The PL spectra was excited using the 351.11 nm line of an Ar^+ laser. The

[11] G. Grem, and G. Leising, Synth. Met. **57**, 4105 (1993).
[12] S. Tasch, A. Niko, G. Leising, and U. Scherf. Appl. Phys. Lett. **68**, 1090 (1996).
[13] S. Tasch, E.J.W. List, O, Ekstroem, W. Graupner, G. Leising, P. Schlichting, U. Rohr, Y. Geerts, U. Scherf, K. Muellen, Appl. Phys. Lett. in print.
[14] S. Tasch, C. Brandstätter, F. Meghdadi, G. Leising, L. Athouel, G. Froyer, Adv. Mat. **9**, 33 (1997).

luminescence radiation was analyzed with a SPEX 0.85 m double monochromator equipped with a cooled GaAs photomultiplier tube and standard photon counting electronics. The Raman measurements were carried out using the 514.5 nm line of an Ar^+ laser. The scattered light was detected with a SPEX triple monochromator equipped with a CCD array detector and a holographic supernotch filter. For low temperature work with DAC a closed cycle refrigerator was employed.

IIIb. Electronic Properties Under High Pressure

Fig. (5) shows the PL and absorption spectra of m-LPPP film at a few selected values of hydrostatic pressure. These measurements were taken at 300 K. The absorption and emission spectra of m-LPPP are governed by the vibronic progression of the order of 0.2 eV, which is indicative of the coupling of the =C-C=C-C= stretch vibration of the conjugated backbone. The vibronic peaks result from the overlap of the wavefunctions of the electronic ground state $|\Psi_{gi}>$ and excited state $|\Psi_{ej}>$, where i and j refer to the vibrational energy levels. The emissive transition which is the highest in energy, is called the 0-0 transition which takes place between the zeroth vibronic level in the excited state to the zeroth vibronic level in the ground state. The 0-1 transition therefore involves the creation of one phonon. There is a Stokes shift between PL and absorption. The 0-0 peak of the absorption is at a slightly higher energy than for the PL. The reason for this shift is that absorption is due to polymer chains of many conjugation lengths (the conjugation length for this sample is about 12) where as PL is from the longest conjugated segments which have lower energies.

Fig. (6) shows the PL spectra of PHP for various pressures. The PL spectra of PHP is also characterized by a vibronic progression. The highest in energy being the 0-0 transition. Owing to self absorption, the high energy edge of the PL emission is strongly affected. This is the reason for the intensity of the 0-0 transition to be lower than the 0-1 transition.

Both m-LPPP and PHP show a red shift in the PL energies on increasing pressure. This red shift has been attributed to an increased intermolecular interaction in the form of a gas-to-crystal[15] effect, where the dipole-dipole interactions with the surrounding medium lowers the excited state energy relative to the ground state. An alternate explanation invokes increased conformational ordering of the polymer chains. Along with the red shift in PL energies, broadening of the peaks is also observed for both m-LPPP and PHP. This has been attributed to the formation of excimers whereby neighboring chains are brought closer together with pressure and hopping of loosely bound electrons between neighboring chain is possible. In this respect both PHP and m-LPPP

[15]R.J. Lacey, D.N. Batchelder, G.D. Pitt, J. Phys. C; Solid State Phys. **17**, 4529 (1984).

behave in a very similar fashion under pressure. Even though m-LPPP has long side chains, it appears that the interchain interaction is increased with pressure.

The main difference in the PL under pressure between the two materials is that PHP under pressure reflects planarization effects. Figure 7 shows the energies of the PL transitions versus pressure in PHP. The strong change in the PL energies which we observe under pressure, below 15 kbar indicates planarization of the molecule in this pressure regime, consistent with our Raman data. The linear pressure coefficient in this regime is ~ -17 meV/kbar which is much larger than what is observed in m-LPPP film (-4 meV/kbar). From our Raman measurements of PHP under pressure the effect of planarization is clearly observed and this is discussed in the following section.

IIIc. Raman Scattering of PHP Under High Pressure

The Raman spectrum of the oligophenyls is mainly characterized by four intense modes of A_g symmetry. It has been observed that the Raman intensity ratio of the inter-ring C-C stretch mode at 1280 cm^{-1} to the C-H in plane bending mode at 1220 cm^{-1} (I_{1280}/I_{1220}) is a good indication for the number of π conjugated phenyl rings in the polymer chain.[16] It is therefore also an indicator for planarity since simulations show that a higher number of conjugated phenyl rings result in a lower torsional angle between the phenyl rings.

Figure 8 shows I_{1280}/I_{1220} for PHP as a function of temperature. This is indicative of structural transition that occurs such that the "averaged" planar confirmation observed at room temperature changes to non-planar at lower temperatures similar to what is observed in lower polyphenyls. The Raman spectrum of PHP shows a frequency shift and a change in I_{1280}/I_{1220} upon increase in pressure as depicted in Fig. 9 and Fig. 10, respectively.

Both the results of temperature- and pressure-dependent Raman studies require that the functional dependence of the potential energy of two neighboring phenyl rings versus torsional angle is W-shaped. Since I_{1280}/I_{1220} is an indicator for *planarity* in these materials, a higher I_{1280}/I_{1220} corresponds to a lower planarity. Lowering the temperature leads to an increase of I_{1280}/I_{1220} which has to be interpreted as a decrease in planarity. Therefore the molecular structural transition with increased temperature is a promotion of the molecule to a higher energy state which is the more planar configuration. This description does not require a change of the shape of the potential energy. However, on increasing pressure the potential energy curve changes; it becomes narrower and starts losing the "W" shape changing towards a "U". This in turn means that the

[16]G. Leising, T. Verdon, G. Louran and S. Lefrant, Synth. Met. **41**, 279 (1991).

energetic difference (ΔE_{np-p}) between the non-planar and the planar conformation of the molecule decreases with increasing pressure. Our experiment confirms this fact: between 15 and 70 kbar the I_{1280}/I_{1220} ratio remains almost a constant (Fig. 10); furthermore, varying the temperature at 20 kbar does not result in any change of the I_{1280}/I_{1220} - both facts indicating that maximum planarity is reached. The former observation shows that the U-shaped potential is already reached at 15 kbar and even by increasing the temperature no further planarization is possible. This is consistent with the PL data of PHP under pressure.

IV. Polarized Photomodulated Reflectivity And Photoluminescence Studies Of Ordered $InGaP_2$

In spontaneously ordered ternary alloys grown on misoriented substrates ordering induced band gap reduction, and valence band splittings exhibiting novel polarization properties have been investigated by theory and experiment. We studied polarized photomodulated reflectivity (PR) and photoluminescence (PL) studies of MOCVD grown $InGaP_2$ epilayers lattice-matched to a GaAs substrate. These structures were grown on a (001) face with a misorientation of two degrees along <110>. The high degree of ordering has enabled us to accurately measure the crystal field splitting and additional structure not reported in the PR spectra. For the electric field E parallel to [110] two features in the PR spectra are seen; for $E \parallel [\bar{1}10]$, however, additional features are observed. A comparison with the spectra of disordered samples of the same alloy composition has enabled a determination of the band gap reduction due to ordering. The linewidths of the PR peaks are approximately 5-10 meV which has enabled us to study them in detail as a function of hydrostatic pressure at cryogenic temperatures. The pressure dependence is slightly sublinear with the first order term of 8-9 meV/kbar for pressures well below the Γ-X crossover. Also observed is the indirect level crossing which occurs under pressure at about 40-kbar. A comparison of PR lineshapes at 1-bar was also studied at several commonly used experimental temperatures. The data indicate a substantial change in PR lineshapes.

The $InGaP_2$ epilayers studied here were both grown by OMVPE techniques at Sandia National Laboratories. The samples are grown lattice-matched to GaAs substrates by using a mole fraction of $Ga_{0.52}In_{0.48}P$. This gives a lattice mismatch of less than 0.1%. The first of the samples is a

disordered (η=0) alloy epilayer with thickness 1.5-μm grown at a temperature of 775°C. The GaAs substrate for this sample is misoriented at an angle θ_B=6° toward $<111>_B$. The second sample is an ordered alloy epilayer with a thickness of 1-μm grown at a low growth rate (~0.5-μm/hr) at a temperature of 675°C. The GaAs substrate for this sample is misoriented at an angle of θ_B=2° toward the $[0\bar{1}1]$ direction off the (001) plane. Under this second set of conditions, samples have been produced with ordering parameters[17] up to $\eta \approx 0.5$ to 0.6.

In the reflectivity experiments, the light is incident to the sample at a small angle (<10°) and is polarized either parallel or perpendicular to the $[\bar{1}10]$ direction, where $[\bar{1}10]$ is the projection of the $[\bar{1}11]$ or $[1\bar{1}1]$ ordering axis on the (001) sample surface. It should be noted here that only these two variants, termed $CuPt_B$, have been seen experimentally in ordered $InGaP_2$ samples[18].[9] When the polarized light has $\mathbf{E} \parallel [\bar{1}10]$, the PR spectrum will display a strong $E_g+\Delta_c$ transition in comparison to E_g, while with $\mathbf{E} \parallel [110]$, the $E_g+\Delta_c$ related transition is very weak according to the selection rules.

The PL spectra of the ordered and disordered $InGaP_2$ samples at 6.5-K, 80-K, and 300-K are shown in Figure 11. We compared the PR spectra at three temperatures for the ordered sample for $\mathbf{E} \parallel [\bar{1}10]$ and $\mathbf{E} \parallel [110]$ polarizations. The PL spectra show a strong peak at 6-K due to the direct gap energy E_g. A shoulder appears at higher temperatures in both the ordered and disordered samples, presumably due to extrinsic features. At low temperatures, the E_g transition in the ordered sample is consistently 100±2-meV lower in energy than that in the disordered sample, leading to an ordering parameter η=0.56±0.03.

The PR spectra for the ordered sample show a pronounced polarization dependence. The transitions sharpen and show temperature dependent intensity. For $\mathbf{E} \parallel [110]$, the data can be fit by one oscillator at 6-K whose energy is identical to E_g measured from PL. At 80-K, a high energy peak (~8 to 10-meV) appears as in the shoulder in PL. Hence the $\mathbf{E} \parallel [110]$ data yields the same results as PL. However, the $\mathbf{E} \parallel [\bar{1}10]$ is rather rich in details. Even at 6-K, a second transition at

---

[17] Alonso R.G., Mascarenhas A., Horner G.S., Bertness K.A., Kurtz S.R., Olson J.M., *Phys. Rev.* B48, 11833 (1993).
[18] Gomyo A., *J. Cryst. Growth* 77, 367 (1986); Gomyo A., Suzuki T., Iijima S., *Phys. Rev. Lett.* 60, 2645 (1988).

about 15-meV higher in energy is resolved. This peak is resolved at 80-K but gets merged with the higher energy $E_g+\Delta_c$ transition at 300-K. The origin of this new feature is not clear at present. It may be due to inhomogeneous in-plane strains due to substrate misorientation or due to variations in ordering variants ($CuPt_A$).

The $E_g+\Delta_c$ transition which is not seen at 6-K due to Boltzmann effects, grows in intensity with increased temperature. At 80-K, it is clearly resolved from the E_g and the second peak described earlier. From the value of Δ_c=36±3-meV, we obtain η=0.59±0.03 which is in good agreement with the ordering induced band-gap reduction.

Figure 12 shows the PR spectra at selected pressures measured in this experiment. Pressure data was obtained at 80-K in all cases. The solid lines through the data in each frame represent the fit to the data. At each pressure, a spectrum was taken at polarizations with $\mathbf{E} \parallel [\bar{1}10]$ and $\mathbf{E} \parallel [110]$. At lower pressures, the spectra are very similar to the 1-bar data. In the spectrum marked 34.3-kbar with $\mathbf{E} \parallel [110]$, a small feature, E_X, appears on the high energy side of the main features. This feature is associated with the indirect-gap transition from the valence band maximum to the X conduction band minimum. As the pressure increases, this transition reduces in energy while the direct gap transitions increase in energy. When the energies of these levels cross, there is a drastic decrease in intensity in the direct gap related spectral features. We have tracked all of these transitions as a function of pressure. The results are plotted in Figure 13. In this figure, the graph shows the energies obtained from the $\mathbf{E} \parallel [\bar{1}10]$ and $\mathbf{E} \parallel [110]$ polarizations in separate frames, providing the pressure dependence of the E_g and $E_g+\Delta_c$ transitions, along with the peak attributed to the indirect transition, labeled E_X. The lines through all data are due to a least-squares fit to a second-order polynomial as in the PL data. The results are summarized in Table (1). We note here that the pressure coefficients for the E_X transition (-2.6±0.1-meV/kbar) is in good agreement with the value calculated for the random alloy, -2.0-meV/kbar and a measured value of -2.5-meV/kbar.

The PL spectra as a function of pressure at 80-K were measured for the ordered $InGaP_2$ sample. Here the E_g transition is seen in both polarizations. The intensity and line-width of the peak is constant up to about 40-kbar, at which a sudden decrease in intensity occurs, and the peak begins to track downward in energy with pressure. This phenomena is consistent with the Γ-X conduction band crossing as has been measured in a previous study, in which high pressure PL

data were compared for samples grown under differing conditions[19]. In Figure (4) (right panel) the peak positions from the PL data are plotted as a function of pressure and fit to a second order polynomial: $E(P)=E_0+\alpha P+\beta P^2$. The values obtained are shown in Table (1). The maximum band gap shift is extrapolated from the data to occur at 40-kbar, with a value of 270-meV. Comparing these values to previous works, we find that our data is in good agreement with a measurement of E_0=1.895 and a maximum shift of about 250-meV at a pressure near 40-kbar. We compare the data in this way as the polynomial fits may not be calculated over the same pressure ranges in all experiments. At pressures above the Γ-X crossover, the peak intensity drops dramatically and could only be tracked to about 51-kbar. The three points in the graph, when fit to a linear function of energy in pressure would give a decrease in energy as 0.6 meV/kbar.[20].

Table I: Pressure Coefficients for $InGaP_2$ Ordered Alloy Sample

Transition E(P=0) (eV)	α meV/kbar	β meV/kbar^2	Method
E_g = 1.900±0.002	8.78±0.02	–0.046±0.007	PL
E_g = 1.900±0.002	7.63±0.02	–0.016±0.005	PR
$E_g+\Delta_c$ = 1.934±0.003	7.71±0.03	-0.0017±0.005	PR
$E\|\|[110]$ =1.9114±0.003	7.35±0.05	-0.0005±0.0003	PR
$E\|\|[\bar{1}10]$ = 1.9150±0.003	7.91±0.05	-0.0027±0.0014	PR
E_X = 2.290.010	-2.63±0.05		PR

V. A comparative study of ordered and random alloy quantum wells of $Zn_{1-x}Cd_xSe/ZnSe$ under pressure

Excitonic transitions in random alloy and ordered alloy quantum wells of $Zn_{1-x}Cd_xSe/ZnSe$

[19] Kobayashi T., and Deol R.S., *Appl. Phys. Lettl* 58, 1289 (1991).
[20] Aspnes D.E., *Surface Science* 37, 418 (1973).

were studied as a function of hydrostatic pressure at 14K using photoluminescence. A sample of bulk $Zn_{1-x}Cd_xSe$ is also studied in the same pressure loading as the other two samples to determine the increase in the bandgap as a function of pressure. This simultaneous study has allowed us to isolate the pressure induced changes due to quantization effects, as well as to study the differences between the random and ordered alloy quantum well systems. We find that the influence of ordering in these samples is evident at thicknesses of ~25Å and less. We also find that a single period of the ordered alloy behaves quantum well like, despite with large overlap of the wavefunction with the barrier and extremely large confinement energy.

Wide band gap II-VI systems have been of considerable interest due to their application in blue-green diode lasers[21,22]. Quantum wells of both ordered and random alloys have been grown in recent years. The quantum wells of these materials, even those single monolayer in thickness, are highly luminescent. However, the efficacy of theoretical models such as tight binding and finite element techniques in the calculation of their energy levels is not yet known, in part because of the limits imposed by the envelope function approximation. For example, it is not clear if the wavefunction overlap between well and barrier are the same in random and ordered alloys for narrow wells of equal thickness. Some of these parameters are best elucidated by tuning an external thermodynamic parameter such as hydrostatic pressure.

In order to study these issues, we have studied under pressure the excitonic transitions in both random alloy and ordered alloy quantum well samples. The random alloy sample of $Zn_{0.75}Cd_{0.25}Se/ZnSe$ has single quantum wells of widths of 25, 50 and 150Å, separated by wide barriers of 450Å. The ordered alloy sample consists of wells formed by repeated periods of [3 monolayer ZnSe / 1 monolayer CdSe] grown on a <100> oriented GaAs substrate, with an effective alloy concentration of x = 0.25, and a 1 period thickness of ~10Å. The wells are formed by 1,2, 4, and 7 periods, giving four quantum wells on the same substrate[23]. As is typical in the ordered alloys, the degree of ordering is not perfect. Due to the sticking coefficient of Se, the coverage in these samples is ~60%, leading to wells that are thinner than expected from the monolayer thicknesses. For a 4 period well, the thickness is 60% x4 periods x 10 Å, ~24Å, while that of the 7 ml well is about 42Å. Thus the 4 ml and 7 ml ordered alloy wells are comparable in thickness to the 25 and 50Å wells in the random alloy quantum well sample. As a baseline sample

[21] M. A. Haase, J. Qiu, J. M. DePuydt and H. Cheng, Appl. Phys. Lett. **59**, 127. 2 (1991).
[22]. H. Jeon, J. Ding, W. Patterson, A. V. Nurmikko, W. Xie, D. C. Grillo, M. Kobayashi, R. L. Gunshor, G. C. Hua and N. Otsuka, Appl. Phys. Lett. **59**, 3619 (1991) and Appl. Phys. Lett. **60**, 2045 (1992).
[23]. H. Luo, N. Samarth, A. Yin, A. Pareek, M. Dobrowolska, J.K. Furdyna, K. Mahalingam, N. Otsuka, F.C. Perris, and J.R. Buschert, J. Electronic Materials, **22**, 467 (1993).

that can be used to subtract the band gap dependence with pressure, we have studied in the same pressure loading as the two quantum well samples a random alloy bulk $Zn_{0.73}Cd_{0.27}Se$ sample[24]. This random alloy sample is 1μm thick, and is assumed to be free standing.

The energies of the transitions as a function of pressure for all three samples is shown in Fig. 14. All the energies were fit using a non linear fits of the type $E(P) = E_o(P) + \alpha P + \beta P^2$, where P is the pressure in kbar. The pressure coefficients obtained are shown in Table II.

It is apparent from Fig. 14 and Table II that the pressure coefficients of the quantum well structures are higher than that of the bulk sample. Several factors influence the energies of the transitions as a function of pressure: changes in the inter-layer strain, which affects the energy of the valence band edge, changes in the quantum confinement energies due to associated changes in the well width and effective masses, changes in the excitonic binding energies due to the effective masses and dielectric constant, and penetration of wavefunction into the barrier, which, in this case, has a higher pressure coefficient. A full scale k.p calculation for all well widths is currently in progress, however, the essential orders of magnitude of the effects may be obtained from looking at a few of the large effects.

In the $Zn_{1-x}Cd_xSe/ZnSe$ structures, the lattice mismatch between the well and the barrier is fairly large. At x = 0.25, the compressive in-plane lattice mismatch strain between well and barrier, $\frac{a_w - a_b}{a_b} = -0.018$. Including an 82:18 CB:VB offset ratio, which is usually used for this system, the depths of quantum wells, calculated using the 8 band k.p technique, are 222 meV in the CB, 93 meV in the heavy hole VB and 8 meV in the light hole VB. Under pressure, due to the differences in the elastic constants in the well and barrier, a pressure induced biaxial tensile strain develops, so that the well and barrier approach lattice match. This happens, however, at a much slower pace than those observed in epilayers of II-VI materials on III-V substrates such as ZnSe/GaAs[25,26,27] or ZnTe/InSb[28]. At 60 kbar, the depth of the HH VB *decreases* by about 2 meV,

---

[24] The concentration of this sample was determined by assuming an exciton binding energy of 0.22 eV, and fitting its luminescence energy of 2.4416 eV at 10 K and P = 0 to the equation $E_g(Zn_{1-x}Cd_xSe) = 2.82 - 1.39x + 0.35\ x^2$, from Brasil et. al, Appl. Phys. Lett,**59** 1026 (1991).

[25] L.J. Cui, U. Venkateswaran, B. A. Weinstein, B.T. Jonker, Phys. Rev. B **44**, 10949 (1991).
[26] B. Rockwell, H.R. Chandrasekhar, M. Chandrasekhar, A. K. Ramdas, M. Kobayashi and R. L. Gunshor, Phys. Rev. **B 44**, 11307 (1991).
[27] J. A. Tuchman, S. Kim, Z. Sui and I. P. Herman, Phys. Rev. **B 46**, 13 371 (1992).
[28] R. J. Thomas, M. S. Boley, H. R. Chandrasekhar, M. Chandrasekhar, C. Parks, A. K. Ramdas, J. Han, M.Kobayashi and R. L. Gunshor, Phys. Rev. B **49** 2181 (1994).

which would contribute to a corresponding *increase* in the transition energy of the quantum well transition as compared to the bulk.

In order isolate the changes in the quantum confined systems from those due to the opening of the band gap with pressure, we plot in Fig. 15 (a) the differences between the transition energies of the quantum wells and the bulk as a function of pressure. The widest quantum well, which is the 150Å random alloy quantum well, increases in energy about 20 meV faster than the bulk over the 60 kbar pressure range. The random alloy quantum well of width 50Å also increases in energy at about the same rate as the 150Å well, showing no more than a deviation of ± 2 meV in energy shift as compared to the 150Å. The 25Å quantum well, however, shows an increase in energy of about 5 meV over the 150Å well (or 25 meV over the bulk) in the same pressure range. This is consistent with our previous study[29] of the PL in ZnCdSe quantum wells under pressure, where effects of pressure dependence on confinement was smaller than those observed in the GaAs/AlGaAs system, and appeared marked in wells of width 50Å or less.

Examining the ordered alloy system, we find that the increase in energy over the bulk for the 7, 4, 2 and 1 period quantum wells at 60 kbar is, respectively, 20, 20.2, 32.8 and 43.8 meV, leading to consequently higher pressure coefficients for the low period wells. In order to compare the random alloy quantum wells with the ordered alloy wells, we look at the energy differences between two pairs of random and ordered alloy wells of approximately the same thickness, viz, the 7 period and the 50Å well pair and the 4 period and the 25Å well pair. These energy differences are plotted in Fig 15 (b). We find that the differences between the 7 period and 50Å well over the pressure range is almost zero. This indicates that the 7 period well behaves pretty much as if it were a random alloy well. With a coverage of 60%, by the time seven periods of the ordered alloy are deposited, the CdSe and ZnSe layers are sufficiently intermixed that the electron wavefunction sees little difference between random and ordered alloys. This is also borne out in the similarity in the pressure coefficients for the 150 and 50 Å random alloy wells and the 7 period (effectively 42Å) ordered alloy well.

The difference between the second pair, the 4 period ordered alloy well and the 25Å well, however, is larger: about 3 meV over the 60 kbar range. While this number is small, the error in it is also small, of the order of ± 10%, due to the direct comparison of the energies of the random and order alloy samples in the same pressure cell, which removes uncertainties due to temperature, pressure calibration, etc. These uncertainties would totally overwhelm these small differences if we were looking at data from two separate measurements.

---

[29] R. J. Thomas, H. R. Chandrasekhar, M. Chandrasekhar, N. Samarth, H. Luo, J.K. Furdyna, Phys. Rev. B **45** 9505 (1992)

The pressure coefficients of the one and two period ordered alloy wells, in contrast, are considerably higher when compared to their wider counterparts. The narrow period wells are, indeed, rather surprising. The one period well is, in structure, merely one monolayer of CdSe buried in a wide layer of ZnSe. One might expect Cd to merely act as an impurity in ZnSe. Its excitonic transition energy is only about 20 meV below the excitonic transition in bulk ZnSe. However, its pressure coefficient is considerably lower than that of bulk ZnSe (6.47 meV/kbar, see Table II). With the one and two period quantum wells, we expect that the well is CdSe like, indicating extremely deep wells, and large interlayer strain. Despite the deep wells, the strong confinement brings the electronic and hole wavefunctions close to the top of the well, as indicated by the energy of the transition. This would cause a large spillover of the wavefunction into the barrier region, thereby allowing much of the wavefunction to take on the larger pressure coefficient of the barrier and therefore the higher pressure coefficient. In addition, the interlayer strain may decrease at a faster rate, being more CdSe-like, which would also contribute to increasing the pressure coefficient. Thus one would expect the ordered alloy quantum wells to have a larger pressure coefficient than the random alloy counterparts of the same width. We also conjecture that the effects of increasing effective mass will be stronger in the narrow wells that are more CdSe-like, and therefore characterized by narrower gaps where band masses increase rapidly. In contrast, in the wider gap ZnCdSe, the band masses do not change very much with pressure.

At the present time, no calculations are available enable us to pinpoint the differences in the electron and hole wavefunctions between the random and ordered alloy wells. We are currently performing calculations using the eight band k.p technique to calculate the energies of the random alloy quantum wells. The ordered alloy system, however, does not lend itself quite as easily to calculations due to the aperiodic nature induced by the effects of layer coverage.

Table II. Pressure coefficients of bulk $Zn_{1-x}Cd_xSe/ZnSe$, and quantum wells of random and ordered alloys of $Zn_{1-x}Cd_xSe/ZnSe$.

Sample		Pressure range (kbar)	Energy (eV)	α (meV/kbar)	β (meV/kbar^2)	Re
Bulk alloys						
	x = 0	0 – 60 kbar	2.7971	6.47 ± 0.19	– 0.0077 ± 0.003	a
	x = 0.14	0 – 110 kbar	2.6152	6.4 ± 0.3	– 0.016 ± 0.003	b
	x = 0.27	0 – 64 kbar	2.4402 eV	6.2 ± 0.2	– 0.016 ± 0.003	
Random alloy quantum wells						
x = 0.18	L_z = 200Å	0 – 60 kbar	2.5565	5.52 ± 0.04		a
	L_z = 60Å	0 – 60 kbar	2.597	5.56 ± 0.03		a
	L_z = 30Å	0 – 60 kbar	2.6489	5.62 ± 0.03		a
x = 0.22	L_z = 30Å	0 – 105 kbar	2.6132	5.64 ± 0.03	–0.005 ± 0.002	b
x = 0.25	L_z = 150Å	0 – 64 kbar	2.5817	5.32 ± 0.04		
	L_z = 50Å	0 – 64 kbar	2.6138	5.28 ± 0.05		
	L_z = 25Å	0 – 64 kbar	2.6652	5.32 ± 0.06		
Ordered alloy quantum wells [3 ml ZnSe / 1 ml CdSe, 60 % coverage]						
7 period	(L_z =~42Å)	0 – 64 kbar	2.6391	5.32 ± 0.05		
4 period	(L_z =~24Å)	0 – 64 kbar	2.6768	5.33 ± 0.05		
2 period	(L_z =~12Å)	0 – 64 kbar	2.7354	5.54 ± 0.06		
1 period	(L_z =~6Å)	0 – 64 kbar	2.781	5.73 ± 0.06		

a. R. J. Thomas et. al Phys. Rev. B 45 9505 (1992). Data taken at 80K.

b.M.S. Boley, Ph.D. Thesis, University of Missouri , 1993.

Sec. VI. Publications arising from this grant

The work supported by this grant has been published/ been submitted to the following journals:

1. Pressure tuning of strain in CdTe/InSb epilayer: photoluminescence and photomodulated study, M.S. Boley, R.J. Thomas, M. Chandrasekhar, H.R. Chandrasekhar, A.K. Ramdas, M. Kobayashi and R.L. Gunshor, J. Appl. Phys, 74, 4136 (1993).

2. Raman and Photomodulated reflectivity studies of strained pseudomorphic ZnTe epilayer on InAs under pressure, R.J. Thomas, M.S. Boley, H.R. Chandrasekhar, M. Chandrasekhar, C. Parks, A.K. Ramdas, J. Han, M. Kobayashi and R.L. Gunshor, Phys. Rev. B 49, 2181 (1994).

3. Hydrostatic Pressure studies of Optical Transitions in the Photoluminescence spectra $Zn_{1-x}Cd_xSe$ thick epilayers and $Zn_{1-x}Cd_xSe$ /ZnSe strained layer multiple quantum wells, M.S. Boley, M. Chandrasekhar, H.R. Chandrasekhar, L.R. Ram-Mohan, N. Samarth, H. Luo, and J.K. Furdyna, Proceedings of the AIRAPT/APS International Conference on High Pressure Science and Technology, June 28-July 2, 1993, Colorado Springs ed. S.C. Schmidt, J.W. Shaner, G.A. Samara, and M. Ross, AIP Conference Proceedings 309, p.203.

4. Raman and Photomodulated reflectivity studies of ZnTe/InAs semiconductor heterostructure under hydrostatic pressure, R.J. Thomas, M.S. Boley, H.R. Chandrasekhar, M. Chandrasekhar, A.K. Ramdas, M. Kobayashi and R.L. Gunshor, Proceedings of the AIRAPT/APS International Conference on High Pressure Science and Technology, June 28-July 2, 1993, Colorado Springs ed. S.C. Schmidt, J.W. Shaner, G.A. Samara, and M. Ross, AIP Conference Proceedings 309, p.613.

5. Optical studies of strained pseudomorphic semiconductor heterostructures under external pressure, M. Chandrasekhar and H.R. Chandrasekhar, invited review article Phil. Mag.B 70, 369 (1994).

6. A comparative study of ordered alloy and Random alloy quantum wells of $Zn_{1-x}Cd_xSe$ /ZnSe under pressure, E.M. Baugher, M. Chandrasekhar, H.R. Chandrasekhar, H. Luo, J.K. Furdyna and L.R. Ram-Mohan, J. Phys. Chem. Solids 56 323 (1995).

7. Polarized photomodulated reflectivity and photoluminescence studies of ordered $InGaP_2$ under pressure, R.J. Thomas, H.R. Chandrasekhar, M. Chandrasekhar, E.D. Jones, and R.P. Schneider, J. Phys. Chem. Solids 56 357 (1995).

8. Polarized Optical studies of Ordered $InGaP_2$ under pressure, R.J. Thomas, H.R. Chandrasekhar, M. Chandrasekhar, E.D. Jones, and R.P. Schneider, Superlattices and Microstructures 18, 1, (1995).

9. Temperature dependence of strain in ZnSe/GaAs, R.J. Thomas, B.A. Rockwell, H.R. Chandrasekhar, M. Chandrasekhar, A.K. Ramdas, M. Kobayashi and R.L. Gunshor, J. Appl. Phys. 78, 6569 (1995).

10. Electrochemically assembled Quasi-periodic quantum dot arrays, S. Bandyopadhyay, A.E. Miller, H.C. Chang, G. Banerjee, V. Yuzhakov, D-F Yue, R.E. Ricker, S. Jones, J.A. Eastman, E. Baugher, and M. Chandrasekhar, Nanotechnology, 7, 360 (1996).

11. Temperature dependence of interband transition in short period GaAs/AlAs superlattices, S. Guha, Q. Cai, M. Chandrasekar, H.R. Chandrasekhar, H. Kim, A.D. Alvarenga, R. Vogelgesang, A.K. Ramdas and M.R. Melloch, Physics of Low-Dimensional Structures **11/12**, 57-62 (1997).

12. Band Gap tuning in Semiconductors and Microstructures, H.R. Chandrasekhar and Meera Chandrasekhar, invited review atticle to be published in Wiley Encyclopaedia of Electrical and Electronics Engineering submitted 1997.

13. Structural properties of poly (para-phenylenes) under high pressure, S.Guha, W. Graupner, R. Resel, M. Chandrasekhar, H.R. Chandrasekhar, and G. Leising, Proceedings of the Materials Research Society, 1997.

14. Electronic properties of poly (para-phenylenes) under high pressure, W. Graupner, S.Guha, S. Yang, M. Chandrasekhar, H.R. Chandrasekhar, G. Leising, U. Scherf, and K. Müllen, Proceedings of the Materials Resesarch Society Fall Meeting, 1997.

15. Temperature dependence of the intervalley deformation potential of GaAs/AlAs superlattices under hydrostatic pressure, S. Guha, Q. Cai, M. Chandrasekhar, H.R. Chandrasekhar, H. Kim, A.D. Alvarenga, R. Vogelgesang, A.K. Ramdas, and M.R. Melloch, Proceedings of the Materials Resesarch Society Fall Meeting, 1997.

16. Photoluminescence of short poeriod superlattices: a hydrostastic pressure and temperature study, S. Guha, Q. Cai, M. Chandrasekhar, H.R. Chandrasekhar, H. Kim, A.D. Alvarenga, R. Vogelgesang, A.K. Ramdas, and M.R. Melloch, accepted for publication in to Phys Rev.

17. Influence of intermolecular interactions on the structural properties of para hexaphenyl, S. Guha, W. Graupner, R. Resel, M. Chandrasekhar, H.R. Chandrasekhar, R. Glaser and G. Leising (Submitted to Journal of Chemical Physics).

18. On the planarity of para-Hexaphenyl. S.Guha, W. Graupner, R. Resel, M. Chandrasekhar, H.R. Chandrasekhar, R. Glaser, and G. Leising, submitted to Phys. Rev. Lett.

Sec. VII. Personnel supported by this grant

- Meera Chandrasekhar, P.I., part of summers 1992-95
- Prof. L.R. Ram-Mohan, Worcester Polytechnic Insitute, Consultant (Nov 15, 1992 to Dec 12, 1992) and summers 1993, 1994.
- Eric Baugher, graduate student, on related EPSCoR grant.(1993-1995), M.S. Ausust 1995.
- Chris Jones, graduate exchange student from Western Illinois University (6 weeks, Summer '95)
- Micha Semmler, graduate student, ETH Zurich, partial summer support 1996
- Suchi Guha,post doctoral fellow, partial support 1996.
- Wilhelm Graupner, Assistant Prof. Technische Universitat Graz, Austria, May 1997, visitor, partial support.
- Chris Martin, graduate student, summer 1997.

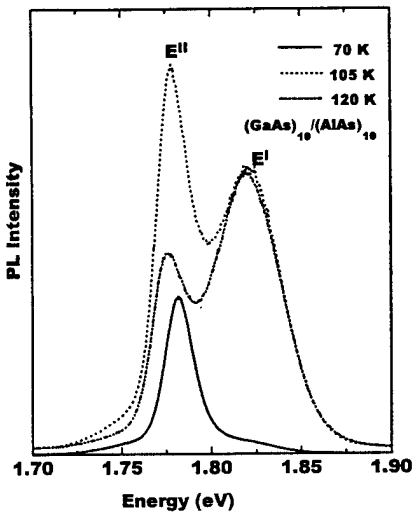

Figure 1: PL spectra of a (10,10) superlattice at three different temperatures (1 bar).

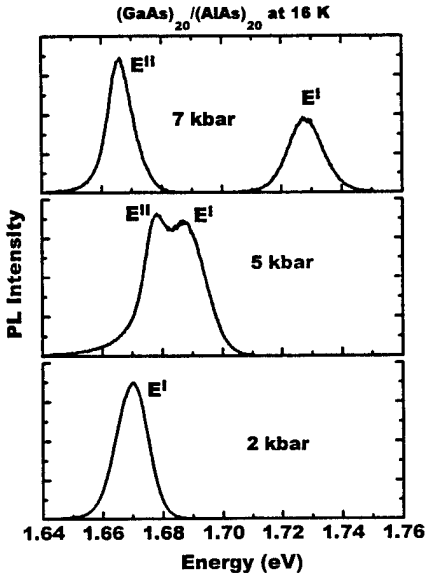

Figure 2: PL spectra of a (20,20) superlattice at three different pressures (16 K).

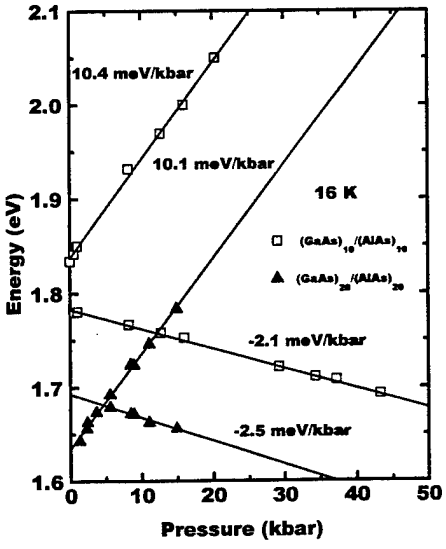

Figure 3: Pressure dependence of the type-I and type-II transitions in $(GaAs)_{10}/(GaAs)_{10}$ (squares) and $(GaAs)_{20}/(GaAs)_{20}$ (triangles) superlattice.

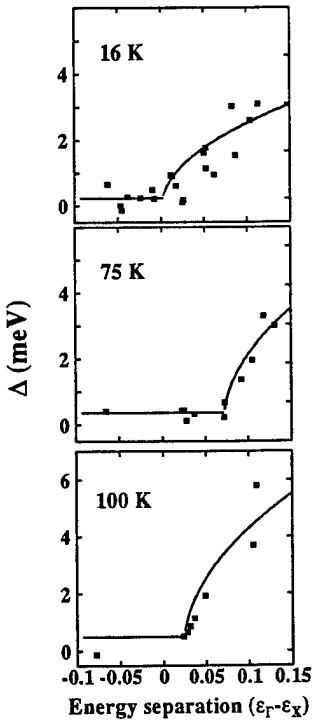

Figure 4: Broadening of the type-I transition versus energy separation between E^{II} and E^{I} for the (20,20) sample, at 3 different temperatures.

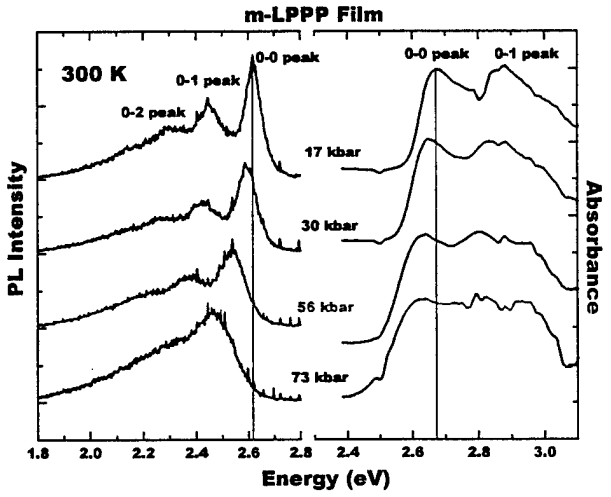

Figure 5: PL and absorption spectra of a m-LPPP film for various pressures and at 300 K

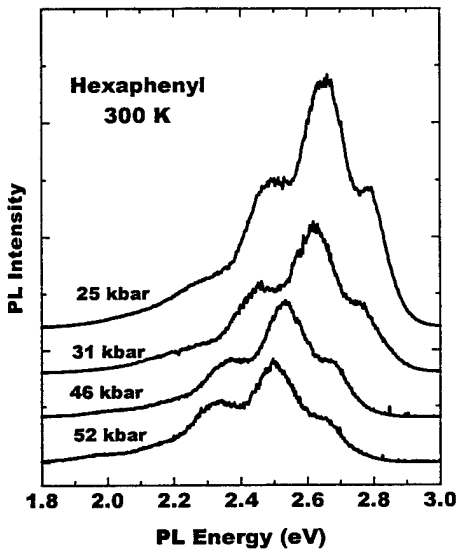

Figure 6: PL Spectra of PHP for various pressures

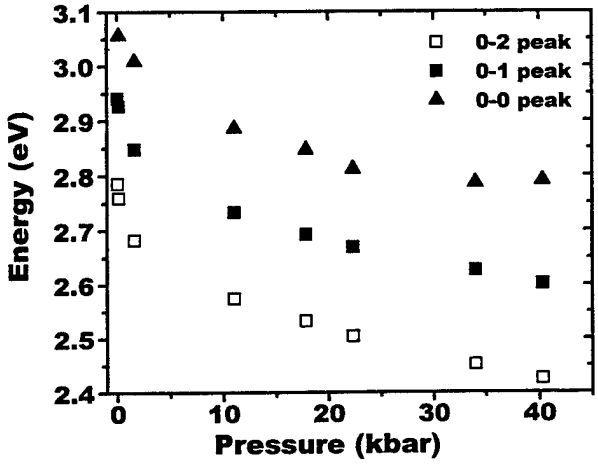

Figure 7: Peak energies of the PL vibronics versus pressure for PHP.

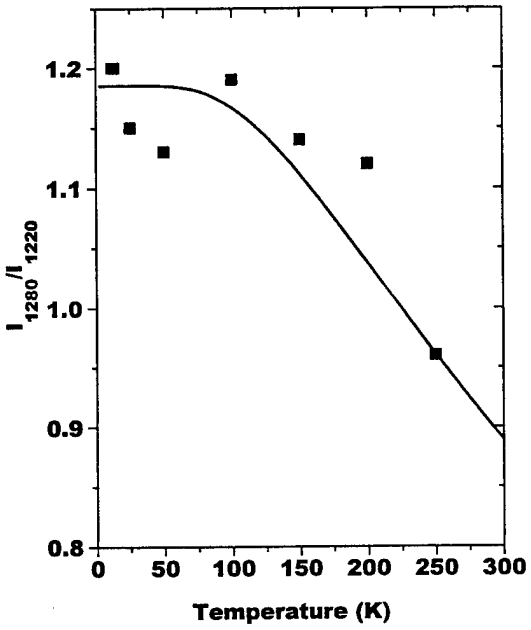

Figure 8: Temperature dependence of the ratio of the Raman modes (I_{1280}/I_{1220}) in PHP.

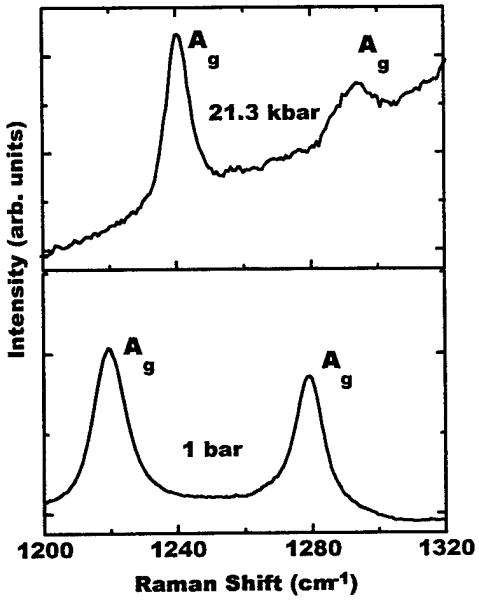

Figure 9: Raman spectra of PHP at 21.3 kbar and at atmospheric pressure.

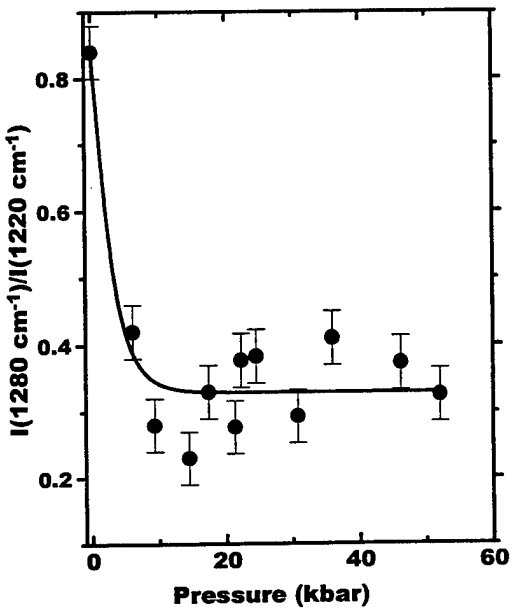

Figure 10: Intensity ratio of the Raman modes (I_{1280}/I_{1220}) as a function of pressure at 300 K.

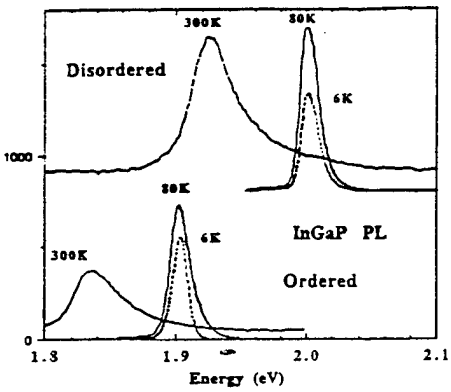

Fig. 11. A comparison of the PL spectra for the ordered and disordered $InGaP_2$ samples at 6, 80, and 300 K.

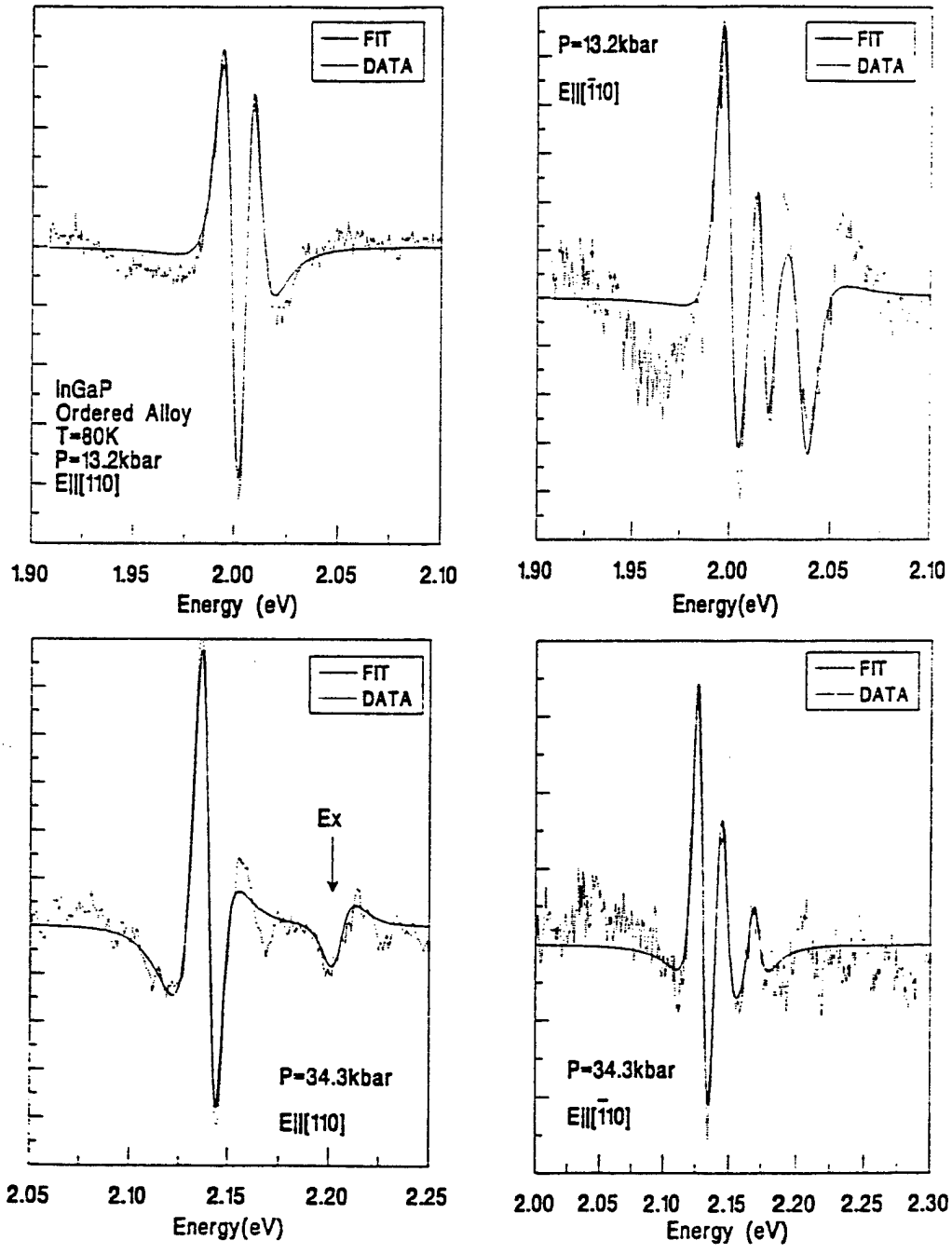

Fig. 12 Polarized PR spectra at selected pressures and at 80 K. The polarizations are indicated. In the 34.3 kbar data with E||[110] the indirect gap transition is indicated by E_x.

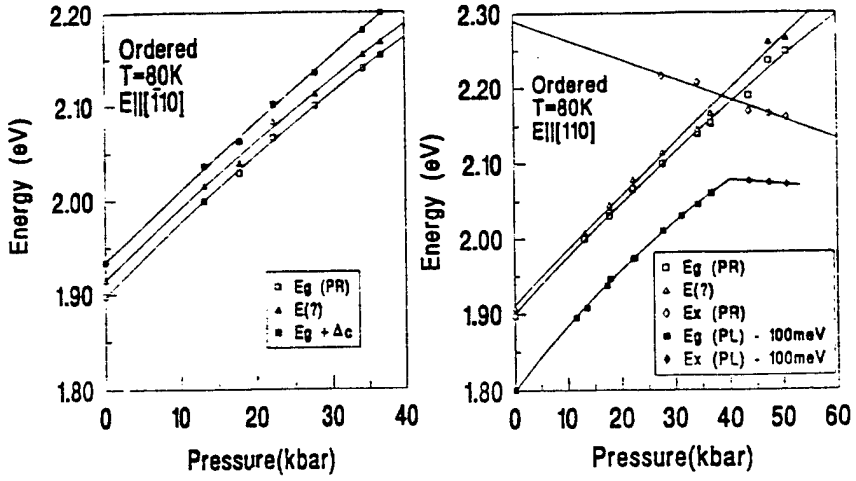

Fig. 13. A summary of the pressure data obtained for the polarized PR and PL experiments at 80 K. The PL data have been included in the frame at the right and have been shifted downward by 100 meV

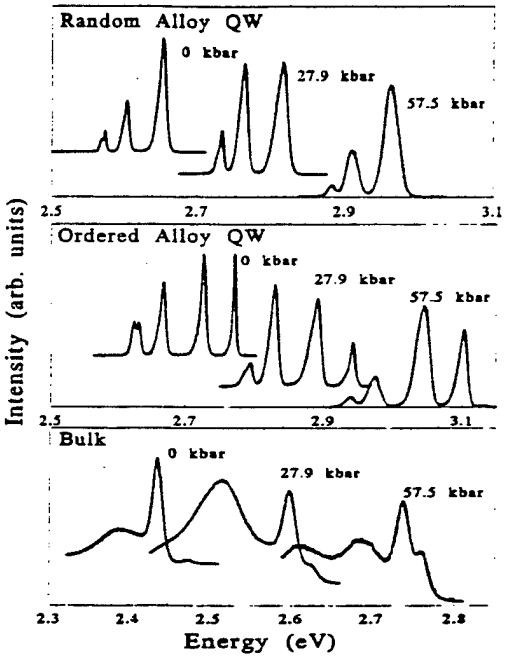

Fig. 14 PL spectra of random alloy quantum wells of widths 25, 50 and 150 Å, ordered alloy quantum wells with 1, 2, 4 and 7 periods, and bulk $Zn_{0.73}Cd_{0.27}Se$ at several pressures.

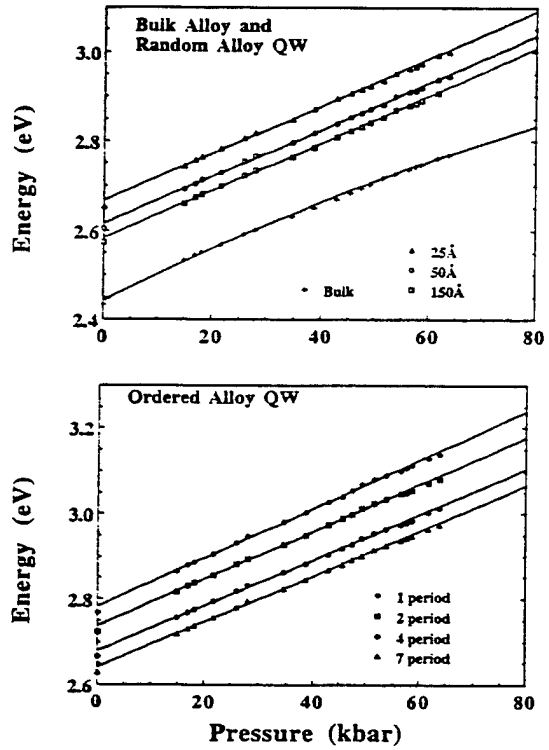

Fig. 16 Energies of the excitonic transitions in the three samples as a function of pressure.

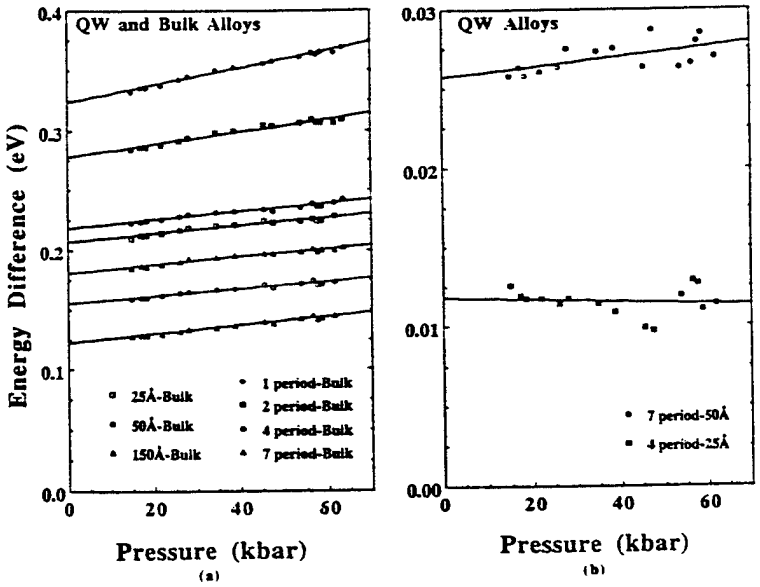

Fig. 15 Differences in transition energies as a function of pressure for several pairs of transitions.